Self-Induced Harmonic Generation in a Storage-Ring Free-Electron Laser

G. De Ninno,[1,2] E. Allaria,[2] M. Coreno,[3] S. Chowdhury,[4] F. Curbis,[2,5] M. B. Danailov,[2] B. Diviacco,[2] M. Ferianis,[2] E. Karantzoulis,[2] E. C. Longhi,[6] I. V. Pinayev,[7] C. Spezzani,[2] M. Trovò,[2] and V. N. Litvinenko[7]

[1]*University of Nova Gorica, Slovenia*
[2]*Sincrotrone Trieste, Basovizza (Trieste), Italy*
[3]*TASC-INFM National Laboratory, Basovizza (Trieste), Italy*
[4]*Xerox Research Center, Webster, New York, USA*
[5]*University of Trieste, Italy*
[6]*Diamond Light Source, Oxfordshire, United Kingdom*
[7]*Brookhaven National Laboratory, Upton, New York, USA*

(Received 18 November 2007; published 10 March 2008)

Coherent radiation from a relativistic electron beam is a valuable way to overcome the present limitations of conventional lasers and synchrotron radiation light sources. The typical scheme has electrons, directly from a linac, in a single-pass interaction with a laser pulse in the presence of a static undulator magnetic field. We demonstrate that a storage-ring free-electron laser can also achieve harmonic generation (down to 36.5 nm), presenting both experimental and theoretical results, and offer a reliable interpretation of the peculiar underlying physical processes involved.

DOI: 10.1103/PhysRevLett.100.104801 PACS numbers: 41.60.Cr, 29.27.−a, 42.60.Jf

Coherent harmonic generation (CHG) using a ''seeded'' relativistic electron beam represents a valuable alternative to self-amplified spontaneous emission (SASE) [1] for obtaining intense, tunable, short-pulse radiation in the wavelength region from the deep ultraviolet down to x rays. The SASE output is typically characterized by very good spatial but limited temporal coherence and large shot-to-shot fluctuations. Harmonic generation potentially provides a drastic improvement of these features [2–4]. The process leading to CHG is based on the frequency upconversion of a high power laser (the seed) through interaction with a relativistic electron beam within an optical klystron [5]. An optical klystron comprises two undulators separated by a dispersive section, the first undulator being referred to as the modulator and the second as the radiator. The seed-electron interaction occurs in the modulator where the electrons exchange energy with the seed pulse. When the beam passes through the dispersive section (e.g., a magnetic chicane), the energy modulation is converted into a spatial microbunching of electrons at the period of the seed wavelength. At the end of the dispersive section the spectrum of electron density has a series of lines at the seed laser frequency and its harmonics. Finally, in the subsequent radiator undulator, light emission at the harmonics of the seed wavelength is enhanced by this coherent bunching and becomes proportional to the square of the number of electrons. In the standard configuration, CHG involves coupling an external laser with the electron bunches extracted from a linear accelerator [6]. Proof of principle experiments were first performed at LURE (Orsay, France) [7] and more recently at Brookhaven Laboratory (Upton, USA) [2,3], where coherent emission at the third harmonic (260 nm) of a Ti:sapphire laser was produced at the end of the radiator. Based on the promising results obtained in [2,3], several projects are currently under development worldwide aiming at the extension of the wavelength range of coherent light sources towards x-ray (see, e.g., [8,9]).

In this Letter, we show that efficient CHG can be obtained from an optical klystron installed in a storage ring (SR) which is used as the interaction region for an oscillator free-electron laser (FEL). In this configuration, the light emitted by the electrons when passing through the undulators is stored in an optical cavity and amplified during successive interactions with the particle beam until lasing is achieved. This intracavity laser signal can provide the seed necessary to initiate CHG [10,11]. Coherent emission in the wavelength range between 260 and 36.5 nm has been observed at the Duke and Elettra SR FELs. We report here experimental results, and provide a reliable theoretical picture of the underlying physical processes. Results indicate that the temporal structure of the harmonic radiation is naturally characterized by very short spikes (hundreds of femtoseconds), in which the majority of the emitted energy is concentrated. This phenomenon, predicted in [12], opens opportunities to exploit CHG in oscillator SR FELs for original user experiments. Alternatively, the radiation produced may be used as the coherent seed in a subsequent single-pass HG scheme.

In a SR, the FEL light originates from spontaneous radiation emitted by the electron beam in the undulators. As a consequence, it is composed of a train of micropulses separated by the interbunch period (hundreds of ns). On a longer temporal scale, laser dynamics are determined by the temporal and spatial overlap of the electron bunch and laser pulse during successive passes through the optical klystron. If perfect overlap is maintained for a few hundred microseconds, a single macropulse is generated, which is the envelope of a train of micropulses (produced on each pass of the electrons through the optical klystron) with

modulated amplitude. Such an envelope will be referred to from now on as a "giant pulse."

The FEL interaction induces an increase of the electron-beam energy spread, i.e., "beam heating." Beam heating in turn causes a concurrent decrease of the FEL gain. Saturation takes place when the gain G is reduced to the level of the losses of the optical cavity, L: $G = L$.

To correctly predict the power generated during the giant pulse, two effects must be considered [12]. The first arises from the synchrotron motion of the electrons during their propagation around the ring. The temporal profile of the FEL gain peaks near the bunch center. Hence, both the FEL radiation intensity and local energy diffusion (heating) grow faster there than at bunch periphery. Synchrotron motion then moves the heated part of the bunch away and brings fresh electrons into the interaction region. This phase-space "refreshment" remains most effective during about half of a synchrotron oscillation (tens of microseconds). After this time, electrons with higher energy spread are evenly distributed through the bunch and the gain is drastically reduced: $G - L$ becomes negative and intensity decays. The second effect requiring consideration comes from the fact that FEL micropulses grow from spontaneous radiation in a process similar to that giving rise to SASE emission. As a consequence, they show a temporal structure composed of very short (i.e., subpicosecond) spikes, with peak power exceeding the local average value by about 1 order of magnitude [13]. The spiky structure of the FEL micropulse significantly increases the effectiveness of phase-space refreshment, further enhancing the FEL peak power.

It has been experimentally demonstrated at the Duke SR FEL [11,14] that enough intracavity power can be produced in the giant pulse regime to induce effective harmonic generation. A suitable manipulation of the light-electron overlap allows the system to be repeatedly brought into this regime through a periodic variation of the tuning condition. Such a variation can be induced either by steering the electron orbit (Duke case [15]), or by changing the beam revolution period (Elettra case [16,17]). Starting from a completely detuned condition, the laser is off, and the electron beam at its minimum energy spread. The light-electron overlap is adiabatically established for the time necessary to generate a single giant pulse (a few hundred microseconds). The system is then detuned again, and after several synchrotron damping times (tens of milliseconds), the energy spread reduces, returning the single-pass FEL gain to its initial (laser-off) maximum value, when the process can be repeated. Figure 1(a) shows a dual-sweep streak camera image of the electron beam and a single giant pulse. As shown in Fig. 1(b), it is possible to generate a stable train of giant pulses. This produces peak power 2 to 3 orders of magnitude higher than the standard steady-state operation mode.

We now describe the basic principles of CHG in a SR FEL. Generally speaking, CHG relies on the production of significant electron bunching at the radiator entrance. Indeed, as seen in Eq. (1), growth of the hth harmonic of the radiated field arises directly from the bunching b_h defined below [18]:

$$\frac{dA_h}{dz} = \frac{1}{N}\sum_{j=1}^{N} \exp[-ih\theta_j(z)] \equiv b_h(z), \qquad (1)$$

where z is the scaled longitudinal coordinate along the undulator axis, A_h $(h = 1, 2, 3, \ldots)$ is the complex hth harmonic component of the scaled field perpendicular to z, and N is the number of electrons. Bunching in the hth harmonic, b_h, is defined in terms of the phase θ_j of the jth electron inside the combined radiation and undulator field. In practice, bunching provides a quantitative measure of the spatial correlation of the particle phase distribution on the scale of the harmonic wavelength λ_h. In a SR FEL, bunching is produced by the interaction of the electron beam with the fundamental field component, A_1, which is stored and amplified in the optical cavity. As previously described, the controlled production of giant pulses provides the seeding signal necessary for the generation of higher harmonics by the following mechanism. At the start of the process (before the giant pulse), the electron distribution is Gaussian in energy with rms value σ_γ, and at the modulator entrance, the electron distribution is generally uniform in phase (i.e., $b_h \simeq 0$ for any h). In the modulator, the light-electron interaction induces a coherent energy modulation, $\Delta\gamma \sin\theta$, of the beam distribution, which overlaps the incoherent energy spread σ_γ. The maximum energy modulation $\Delta\gamma$ is proportional to the seed field, A_1. Bunching is created in the dispersive sec-

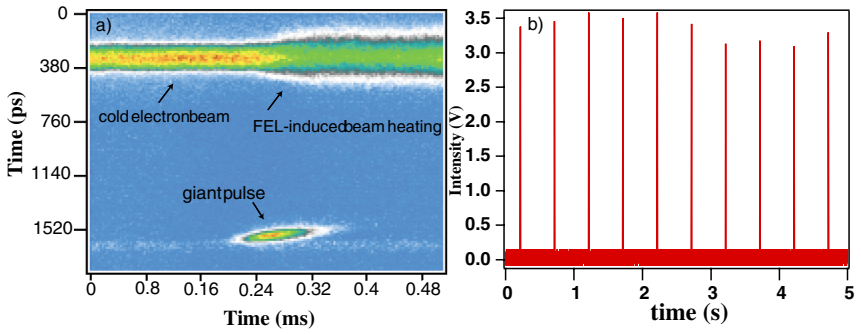

FIG. 1 (color online). (a) Dual-sweep streak camera image (from Duke) of the electron beam (upper) during the generation of a single giant pulse, and the laser signal (lower). A vertical slice of the image gives a snapshot of the electron beam and/or laser temporal distribution. (b) A train of giant pulse laser signals is shown with a 2 Hz repetition rate.

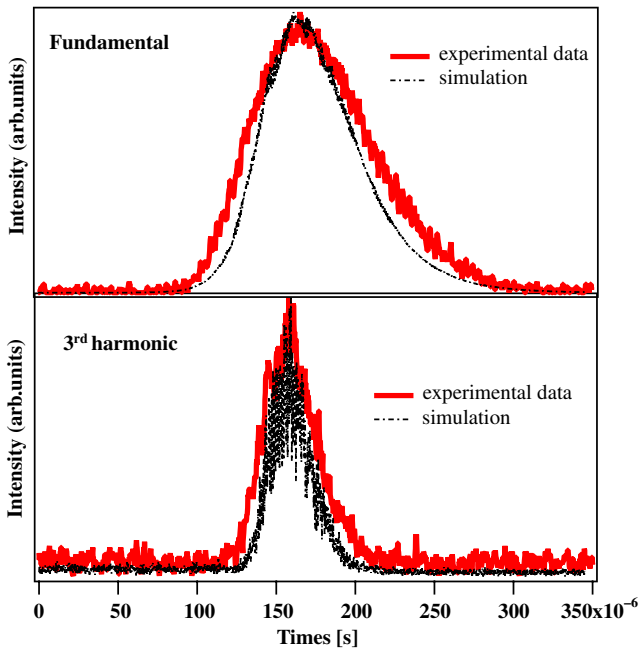

FIG. 2 (color online). Evolution of the laser power in a single giant pulse at 660 nm fundamental (upper) and 220 nm 3rd harmonic (lower). The dotted curves show GINGER prediction for the same experimental parameters. In this case (from Elettra), beam energy: 900 MeV, peak current: 32 A, normalized transverse emittance: ~2.5 μm, laser-off energy spread: ~770 keV (rms), laser-off bunch duration: ~16 ps (rms), cavity losses: 1%, number of undulator periods: 20, undulator length: 2 m.

tion, where the beam energy modulation is transformed into phase modulation: electrons of phase θ_j at the exit of the modulator will have a new phase $\theta_j + \bar{D}x\Delta\gamma \sin\theta_j$ at the entrance to the radiator, where $\bar{D}$ is the (positive) strength of the dispersive section. Therefore, when $\sin\theta_j > 0$ the new phase is smaller than the initial one, while the opposite occurs when $\sin\theta_j < 0$, thus producing particle clustering, i.e., $b_h \neq 0$.

Because of synchrotron motion, after one turn in the SR, the coherent energy modulation is transformed into incoherent energy spread. Turn after turn, the energy spread accumulates. Eventually, the net gain $G - L$ reduces to zero, so that the seed power decays and CHG is suppressed.

Experimental results obtained at Duke and Elettra are now compared with numerical simulations performed using the three-dimensional numerical code GINGER [19]. GINGER solves the coupled system of Newton-Lorentz (for particles) and Maxwell equations (for fields) inside the optical klystron. A separate SR tracking code is used to account for particle motion around the ring. Figure 2 shows the evolution of the fundamental (660 nm) and third harmonic (220 nm) macropulses measured at the Elettra FEL. One can see that the harmonic macropulse is characterized by a shorter rise time than the fundamental giant pulse. A difference of about a factor of 3 has been found, as expected from the theoretical prediction $A_h \propto A_1^h$ [11]. Simulations are in satisfactory agreement with experiments. A similarly good agreement between experimental and numerical results has been found in the case of the Duke FEL, both at the fundamental and third harmonic wavelengths.

The energy of both the fundamental and harmonic micropulses was also measured. In the Duke case, using holed cavity mirrors at 260 nm, and micropulse energy of 3 mJ in the fundamental produced several nJ extracted energy at 86.1 nm (third harmonic) and a fraction of nJ at 51.5 nm (fifth harmonic) and 36.5 nm (seventh harmonic). Experiments at Elettra utilized mirrors at 660 and 450 nm, partially transmitting at 220 and 150 nm (respectively), producing measured micropulse energies of the same order of those generated at Duke, i.e., a few mJ (intracavity) at the fundamental wavelength and few nJ at the third harmonic. These measured energy values are in good agreement with simulation, which showed an accuracy better than 20%.

As mentioned, FEL radiation arises from spontaneous emission by the electrons. Because particle density inside the bunch is inhomogeneous, the emitted micropulse is composed of spikes having various peak powers. The typical duration of a single spike is approximately equal to the "slippage" distance along the optical klystron [20], due to a process analogous to a SASE system. Spiky

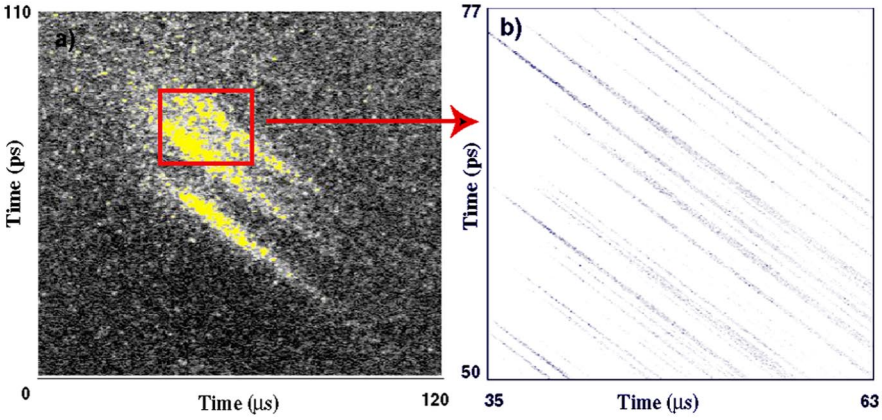

FIG. 3 (color online). (a) Streak camera image (from Duke) of the third harmonic at 233 nm showing micropulses. The slope in the pulse evolution is due to a small detuning of the electron and radiation round-trip times. (b) Numerical streak image produced using GINGER, with the same temporal ranges as figure (a). In this case, beam energy: 780 MeV, peak current: 37 A, normalized transverse emittance: ~15 μm, laser-off energy spread: ~920 keV (rms) laser-off bunch duration: ~100 ps (rms), cavity losses: 1%, number of undulator periods: 33.5, undulator length: 3.35 m.

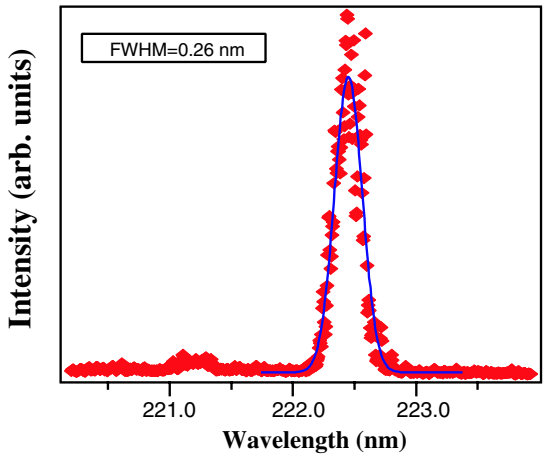

FIG. 4 (color online). Spectrum of the coherent third harmonic at 222.5 nm from Elettra.

micropulses at the fundamental wavelength are stored in the optical cavity and amplified during successive interactions with the electron beam. As a consequence, at the peak of a giant pulse, the majority of the power is concentrated in a few intense isolated spikes, which will be reflected in the temporal structure of the harmonic micropulses. This prediction is confirmed by experiments and simulations, as shown below.

The temporal structure of the FEL micropulse has been investigated using a dual-sweep streak camera. Figure 3(a) shows a streak camera image of third harmonic coherent radiation at 233 nm generated with the Duke FEL. The picture gives a clear indication of the predicted spike structure in harmonic pulses, in this case with a measured duration of about 2 ps (rms). However, this is close to the instrument resolution and underlying finer structure could not be resolved. Simulations at higher temporal resolution confirm the existence of a much finer structure seen in Fig. 3(b), i.e., spikes on the order of a few hundreds of fs (comparable to the Duke FEL slippage in the case under consideration). Using a streak camera of similar resolution, spikes have not been detected at Elettra. This is likely explained by the fact that the Elettra bunch duration (about 20 ps, rms) is significantly shorter than the one at Duke (about 100 ps, rms). As a consequence, the duration of the envelopes of the fundamental and harmonic micropulses will be significantly shorter as well, making spikes unresolvable experimentally. An indirect confirmation of the sub-ps structure of the Elettra harmonic pulses has been obtained by measuring the spectral profile. As an example, Fig. 4 shows a spectrum of the third harmonic at 222.5 nm having a width of 0.26 nm (FWHM). Assuming that the optical spike is transform limited, this corresponds to a temporal duration of 120 fs (rms), which is very close to the value obtained from simulations.

In conclusion, we have shown that when operated in the giant pulse regime, SR FELs can produce intense harmonic radiation in the VUV spectral range. The harmonic micropulses have a sub-ps temporal structure, which may prove to be useful for experiments investigating ultrafast phenomena.

We are grateful to W. M. Fawley for enlightening discussions and technical assistance with GINGER simulations. We also thank Gary Swift, as well as the Duke and Elettra accelerators teams.

*giovanni.deninno@elettra.trieste.it

[1] A. Kondratenko and E. Saldin, Part. Accel. **10**, 207 (1980); Y. Derbenev, A. Kondratenko, and E. Saldin, Nucl. Instrum. Methods Phys. Res., Sect. A **193**, 415 (1982); R. Bonifacio, C. Pellegrini, and L. Narducci, Opt. Commun. **50**, 373 (1984); M. Babzien *et al.*, Phys. Rev. E **57**, 6093 (1998); S. V. Milton *et al.*, Phys. Rev. Lett. **85**, 988 (2000); J. Andruszkow *et al.*, Phys. Rev. Lett. **85**, 3825 (2000); R. Brinkmann, in *Proceedings of the FEL Conference, 2006*, http://www.bessy.de/fel2006/proceedings/PAPERS/MOBAU03.PDF
[2] A. Doyuran *et al.*, Phys. Rev. Lett. **86**, 5902 (2001).
[3] L. H. Yu *et al.*, Phys. Rev. Lett. **91**, 074801 (2003).
[4] E. Allaria and G. De Ninno, Phys. Rev. Lett. **99**, 014801 (2007).
[5] N. A. Vinokurov and A. N. Skrinsky, Budker Institute for Nuclear Physics Report No. BINP 77-59, Novossibirsk, 1977.
[6] L. H. Yu, Phys. Rev. A **44**, 5178 (1991).
[7] B. Girard *et al.*, Phys. Rev. Lett. **53**, 2405 (1984).
[8] E. Allaria *et al.*, in *Proceedings of the FEL Conference 2006*, http://www.bessy.de/fel2006/proceedings/PAPERS/MOPPH054.PDF
[9] A. Mesnek, in *Proceedings of the FEL Conference 2006*, http://www.bessy.de/fel2006/proceedings/PAPERS/MOCAU01.PDF
[10] G. Dattoli *et al.*, J. Appl. Mech. Tech. Phys. **10**, 5034 (1998).
[11] V. N. Litvinenko Nucl. Instrum. Methods Phys. Res., Sect. A **507**, 265 (2003).
[12] V. N. Litvinenko *et al.*, Proc. SPIE Int. Soc. Opt. Eng. **2521**, 78 (1995); V. N. Litvinenko *et al.*, Nucl. Instrum. Methods Phys. Res., Sect. A **375**, 46 (1996).
[13] C. Pellegrini, Nucl. Instrum. Methods Phys. Res., Sect. A **475**, 1 (2001).
[14] E. C. Longhi, Ph.D. thesis, Duke University, 2006.
[15] I. Pinayev *et al.*, Nucl. Instrum. Methods Phys. Res., Sect. A **528**, 283 (2004).
[16] T. Hara *et al.*, Nucl. Instrum. Methods Phys. Res., Sect. A **341**, 21 (1994).
[17] G. De Ninno *et al.*, Nucl. Instrum. Methods Phys. Res., Sect. A **528**, 278 (2004).
[18] W. B. Colson, in *Laser Handbook* (North-Holland, Amsterdam, 1990), p. 115
[19] W. Fawley, LBL Report No. LBNL-49625, 2002.
[20] Slippage is defined as the distance by which an electron lags behind the photons during propagation inside the optical klystron.